Biochimica et Biophysica Acta 1844 (2014) 545–552

Contents lists available at ScienceDirect

Biochimica et Biophysica Acta

journal homepage: www.elsevier.com/locate/bbapap

P-I class metalloproteinase from *Bothrops moojeni* venom is a post-proline cleaving peptidase with kininogenase activity: Insights into substrate selectivity and kinetic behavior

Débora N. Okamoto [a], Marcia Y. Kondo [a], Lilian C.G. Oliveira [a], Rodrigo V. Honorato [b], Leticia M. Zanphorlin [c], Monika A. Coronado [d], Mariana S. Araújo [e], Guacyara da Motta [e], Camila L. Veronez [e], Sheila S. Andrade [f], Paulo S.L. Oliveira [b], Raghuvir K. Arni [d], Adelia C.O. Cintra [g], Suely V. Sampaio [g], Maria A. Juliano [a], Luiz Juliano [a], Mário T. Murakami [b,*], Iuri E. Gouvea [a,**]

[a] Departamento de Biofísica, Universidade Federal de São Paulo, 04044-020 São Paulo, SP, Brazil
[b] Laboratório Nacional de Biociências, Centro Nacional de Pesquisas em Energia e Materiais, 13083-100 Campinas, SP, Brazil
[c] Departamento de Orgânica, Instituto de Química, UNICAMP, 13083-970 Campinas, Brazil
[d] Departamento de Física, IBILCE, UNESP, 15054-000 São José do Rio Preto, Brazil
[e] Departamento de Bioquímica, Universidade Federal de São Paulo, 04044-020 São Paulo, SP, Brazil
[f] Departamento de Ginecologia, Universidade Federal de São Paulo, 04044-020 São Paulo, SP, Brazil
[g] Departamento de Análises Clínicas, Toxicológicas e Bromatológicas, Faculdade de Ciências Farmacêuticas de Ribeirão Preto-USP, 14040-903 Ribeirão Preto, SP, Brazil

ARTICLE INFO

Article history:
Received 7 August 2013
Received in revised form 17 December 2013
Accepted 19 December 2013
Available online 27 December 2013

Keywords:
Snake venom metalloproteinase
Kininogenase activity
FRET peptides
Substrate specificity
Molecular dynamics simulations

ABSTRACT

Snake venom metalloproteinases (SVMPs) belonging to P-I class are able to hydrolyze extracellular matrix proteins and coagulation factors triggering local and systemic reactions by multiple molecular mechanisms that are not fully understood. BmooMPα-I, a P-I class SMVP from *Bothrops moojeni* venom, was active upon neuro- and vaso-active peptides including angiotensin I, bradykinin, neurotensin, oxytocin and substance P. Interestingly, BmooMPα-I showed a strong bias towards hydrolysis after proline residues, which is unusual for most of characterized peptidases. Moreover, the enzyme showed kininogenase activity similar to that observed in plasma and cells by kallikrein. FRET peptide assays indicated a relative promiscuity at its S_2–S'_2 subsites, with proline determining the scissile bond. This unusual post-proline cleaving activity was confirmed by the efficient hydrolysis of the synthetic combinatorial library MCA-GXXPXXQ-EDDnp, described as resistant for canonical peptidases, only after Pro residues. Structural analysis of the tripeptide LPL complexed with BmooMPα-I, generated by molecular dynamics simulations, assisted in defining the subsites and provided the structural basis for subsite preferences such as the restriction of basic residues at the S_2 subsite due to repulsive electrostatic effects and the steric impediment for large aliphatic or aromatic side chains at the S_1 subsite. These new functional and structural findings provided a further understanding of the molecular mechanisms governing the physiological effects of this important class of enzymes in envenomation process.

1. Introduction

Viperidae snakebite envenomation triggers a number of local and systemic physiological responses such as hemorrhage, edema, inflammation, necrosis, fibrinolysis and apoptosis [1]. Some snake venoms can also induce the inhibition of platelet aggregation and the activation of prothrombin and Factor X [2,3]. On the basis of their domain architectures, snake venom metalloproteinases (SVMPs) are classified in three main classes: P-I, which comprises only the metalloproteinase domain; P-II, consisting of metalloproteinase and disintegrin domains; and P-III, which additionally contains a cysteine-rich domain and a C-terminal lectin-like domain [4].

In spite of a number of studies regarding the structure and function of SVMPs, the variety of biological activities and clinical manifestations is not fully understood [1]. The members of class P-I mainly induce local hemorrhage and have lower hemorrhagic potency than P-III SVMPs, probably due to the absence of C-terminal accessory domains [5,6]. To date, the crystal structure of nine P-I SVMPs has been reported [1,7,8]. The last to be structurally characterized was BmooMPα-I, a non-hemorrhagic metalloproteinase isolated from *Bothrops moojeni* venom [7].

BmooMPα-I is a 22.6 kDa P-I SVMP, which displays azocaseinolytic and fibrin(ogen)olytic activities, but is devoid of hemorrhagic activity.

* Correspondence to: M.T. Murakami, Laboratório Nacional de Biociências, CNPEM, Rua Giuseppe Maximo Scolfaro, 10000, Campinas 13083-970, Brazil. Fax: +55 19 3512 1100.
** Correspondence to: I.E. Gouvea, Departamento de Biofísica, UNIFESP — Rua Três de Maio, 100, São Paulo 04044-020, Brazil. Fax: +55 11 5575 9617.
E-mail addresses: mario.murakami@lnbio.cnpem.br (M.T. Murakami), iurig@yahoo.com (I.E. Gouvea).

1570-9639/$ – see front matter © 2014 Elsevier B.V. All rights reserved.
http://dx.doi.org/10.1016/j.bbapap.2013.12.014

Due to its defibrinogenating effect observed in in vivo experiments in mice, BmooMPα-I is of great medical interest as a therapeutic agent in the treatment and prevention of thrombotic diseases [9]. Its crystal structure revealed a novel distorted octahedral coordination of the catalytic zinc ion and the sequence motif tandem to the Met-turn was addressed as the one responsible for the functional differentiation between non- and hemorrhagic P-I class SVMPs [7]. However, the substrate specificity of BmooMPα-I as well as the pH and salt dependences of its proteolytic activity remains unresolved.

Thus, this work aimed to interrogate the putative physiological substrates of BmooMPα-I and to determine its amino acid subsite specificity by FRET peptide assays. Moreover, its kinetic properties were analyzed under different physical–chemical environments and molecular dynamics simulations were employed to gain insights into the structural determinants for substrate recognition and interaction by the subsites.

2. Materials and methods

2.1. Enzyme purification

Crude desiccated *B. moojeni* venom was purchased from SanMaru serpentarium (Taquaral, Sao Paulo, Brazil). The P-Iclass SVMP from *B. moojeni*, named as BmooMPα-I, was purified based on the previously published protocol [7]. The purification steps include anion-exchange chromatography on Q-Sepharose (Amersham Biosciences), size-exclusion chromatography on Superdex 75 (Amersham Biosciences) and affinity chromatography on Heparin-Sepharose (Amersham Biosciences). The purity of the sample was confirmed by sodium dodecyl sulfate polyacrylamide gel electrophoresis (SDS-PAGE) under reducing conditions [10]. Protein concentration was determined by absorbance at 280 nm, using a theoretical extinction coefficient of 24,325 M^{-1} cm^{-1} [11]. Control experiments were performed in the presence of 1 mM of the inhibitor 1,10-phenanthroline.

2.2. Peptide synthesis

All FRET peptides were obtained by the solid-phase peptide synthesis strategy as previously described [12]. An automated bench-top simultaneous multiple solid-phase peptide synthesizer (PSSM 8 system, Shimadzu, Japan) was used to synthesize peptides using the Fmoc-procedure. The molecular mass and purity of the peptide were checked by analytical HPLC and by MALDI-TOF using the mass spectrometer Microflex-LT (Bruker — Daltonics, Billerica, MA, USA). The libraries of FRET peptides were derived from bradykinin (BK) sequence, being the reference Abz-GFSPFRQ-EDDnp, where Abz (ortho-aminobenzoic acid) is the fluorescence donor and Q-EDDnp (glutamine-[N-(2,4-dinitrophenyl)-ethylenediamine]) is the fluorescence acceptor. Variations of amino acids from this reference sequence occurred as: Abz-GF<u>X</u>PFRQ-EDDnp, Abz-GFS<u>X</u>FRQ-EDDnp, Abz-GFSP<u>X</u>RQ-EDDnp and Abz-GFSPF<u>X</u>Q-EDDnp. The peptide series Abz-KLXPSKQ-EDDnp was also synthesized as described above.

2.3. Screening of Abz-GXXXXXQ-EDDnp library

The library was synthesized as described in Oliveira et al. [13]. The reactions were initiated by the addition of the enzyme in the library solutions (final concentration of 6 μM). The reactions were followed over 300 s, and the initial linear increase of fluorescence with time was taken as the rate of hydrolysis, in 50 mM Tris–HCl pH 7.5 buffer with 100 mM NaCl and 10 μM of $ZnCl_2$.

2.4. Stock solutions of peptides

The solutions of all FRET peptides, including Abz library were prepared in DMSO and the concentrations obtained by colorimetric determination of the 2,4-dinitrophenyl (Dnp) group, using $\varepsilon_{365} = 17{,}300\ M^{-1}\ cm^{-1}$. The concentration of DMSO in assay buffers was kept below 1% (*v*/*v*).

2.5. Hydrolysis of FRET peptides

The hydrolysis of FRET peptides and Abz library was monitored continuously using a Hitachi F-2500 spectrofluorimeter, at λ_{ex} 320 nm and λ_{em}420 nm. When using MCA([7-amino-4-methyl]coumarin) as fluorescence donor, the parameters were modified to λ_{ex} 325 nm and λ_{em} 395 nm. The inner-filter effect was corrected as previously described [14]. The scissile bond of peptides was identified by isolation of the fragments using analytical HPLC followed by determination of their molecular mass by LC/MS using an LCMS-2010 equipped with an ESI-probe (Shimadzu, Japan). All the assays were taken in 50 mM Tris–HCl buffer pH 7.5 containing 100 mM NaCl and 10 μM of $ZnCl_2$.

To determine the primed side cleavage specificity, a 100 μM solution of MCA-GXXPXXQ-EDDnp was incubated with BmooMPα-I overnight at 37 °C. Reactions were stopped by heating at 100 °C for 5 min and the N-terminal amino acid sequence was determined by Edman degradation using a Model PPSQ-23 protein sequencer (Shimadzu, Tokyo, Japan). Amino acid preference in a given cycle was calculated by dividing the amount of a particular residue by the amount of prevalent amino acid residue in that cycle. The data were then corrected for bias present in the library by dividing each value by the relative amount of that particular amino acid in the starting mixture.

2.6. Kinetic parameter determination

The kinetic parameters of hydrolysis, k_{cat}, K_M, and k_{cat}/K_M were determined from initial rate measurements at FRET substrate concentrations up to 40 μM. The enzyme concentrations were chosen such that less than 5% of the substrate was hydrolyzed over the course of the assay. The reaction rate was converted into micromoles of substrate hydrolyzed per minute based on a calibration curve obtained from the complete hydrolysis of each peptide. The data were fitted with respective standard errors to the Michaelis–Menten equation using GraFit software version 5.0 (Erithacus Software, Horley, Surrey, U.K.).

When necessary the specificity rate constants (k_{cat}/K_M) were directly determined by dividing the pseudo first-order rate constant by the active enzyme concentration present in the reaction mixture [14]. Pseudo first-order rate constants of hydrolysis were measured at $[S] \ll K_M$ and calculated by nonlinear regression data analysis, using the GraFit software.

2.7. The pH and salt dependence of specificity constant

The pH dependence of rate constants was measured under Michaelis–Menten conditions at 37 °C in a four-component buffer comprised of 75 mM Tris, 25 mM Mes, 25 mM acetic acid and 25 mM glycine, using the fluorimetric assay described above. The data were fitted to the theoretical curve for the bell-shaped pH rate profiles using nonlinear regression as in Eq. (1) using GraFit software:

$$k = \frac{k(\mathrm{Limit})10^{pH-pK_{a1}}}{10^{2pH-pK_{a1}-pK_{a2}}} \quad (1)$$

where k_{cat}/K_M(limit) stands for the pH-independent maximum k_{cat}/K_M constant and K_1 and K_2 are the dissociation constants of the catalytic components at acidic and basic limbs, respectively $k = k_{cat}$ or k_{cat}/K_M.

The influence of NaCl was investigated over a range of 0–1 M, the assays were performed as previously determined using Abz-GFSPFRQ-EDDnp as substrate.

2.8. Cleavage of human high molecular weight kininogen (HMWK) by BmooMPα-I

To analyze HMWK processing by BmooMPα-I, HMWK (1 μg) was incubated with BmooMPα-I (1 and 10 μg) in 50 mM Tris/HCl buffer, pH 7.5 with 10 μM $ZnCl_2$ for 20 min at 37 °C. The reaction was stopped by thermal shock at −80 °C. The samples were boiled after addition of 3% β-mercaptoethanol, resolved by 10% SDS-PAGE and blotted onto a polyvinylidene fluoride (PVDF) membrane (GE Healthcare, UK). The membrane was blocked with 5% (*w*/*v*) skim milk powder in PBS/0.1% Tween 20 and incubated with a rabbit anti-HMWK antibody (1 μg/mL). A second incubation was performed with goat anti-rabbit IgG (peroxidase-conjugated) (1:15,000) (Sigma, USA). HMWK (or its fragments) was detected on the PVDF membrane by visualizing antigen–antibody complexes with chemiluminescence. Intact HMWK was used as a control.

2.9. Radioimmunoassay

The ability of BmooMPα-I to release bradykinin was assayed with HMWK [15]. The enzyme (1 μg) in 50 mM Tris/HCl buffer, pH 7.5 with 10 μM $ZnCl_2$ was incubated with HMWK (1.4 μg) in 40 μl for 5, 10, 15 and 20 min at 37 °C. The kinin was extracted in ethanol (1:4 *v*/*v*) for 10 min at −70 °C. Solutions were freeze-dried and dissolved in 200 μl of 10 mM phosphate buffer, pH 7.0 with 140 mM NaCl, 0.1% NaN_3, 30 mM EDTA, 3 mM 1,10-phenanthroline and 0.1% ovalbumin. 50 μl of the samples was incubated with 100 μl of anti-BK antibody [16] (1:1000) and 100 μl of ^{125}I-labeled Tyr-bradykinin probe, for 20 h at 4 °C. Then, 400 μl of 0.1% bovine γ-globulin in 10 mM phosphate buffer, pH 7.0, 140 mM NaCl, 0.1% NaN_3 and 800 μl of 25% polyethylene glycol 6000 were added to the samples and incubated by 10 min at 4 °C. Samples were centrifuged at 2000 ×*g* for 20 min at 4 °C. The solutions obtained were removed and the pellets were submitted to the radiation counting (Cobra II Auto-Gamma, Packard BioScience, Meriden, CT, USA) and the bradykinin released was determined. Statistical analyses were performed using one-way analysis of variance (ANOVA) followed by Welch's correction.

2.10. Docking and molecular dynamics

The BmooMPα-I structure (PDB ID: 3GBO) [6] and the predicted structure of proposed peptides (LAL, LPL and LWL) were manually docked based on the peptomimetic structure, found in another PI-class SVMP complex (PDB ID: 2W15 [17]). The complex comprising the enzyme, the peptide and two conserved water molecules, involved into the zinc atom coordination, was prepared for energy minimization and molecular dynamics simulation using the program YASARA [18]. The parameters for the force field were obtained from YAMBER3 [19]. The p*Ka* values for Asp, Glu, His and Lys residues were predicted. Based on pH 7.0, the protonation states were assigned according to the following convention: Asp and Glu were protonated if the predicted p*Ka* was higher than the pH; His was protonated if the predicted p*Ka* was higher than the pH and it did not accept a hydrogen bond, otherwise it was deprotonated; Cys was protonated; Lys was deprotonated if the predicted p*Ka* was lower than the pH and; Tyr and Arg were not modified. A simulation cell was defined with a distance of 15 Å from all atoms of the complex with periodic boundaries. Then, the simulation cell was filled with water molecules and Na/Cl ions, which were placed at the lowest/highest electrostatic potential locations, in order to neutralize the cell and obtain a NaCl concentration of 0.9%. A short MD simulation was performed for solvent relaxation, water molecules were subsequently deleted until the system density reached 0.997 g/ml. A short steepest descent EM was carried until the maximum atom speed dropped below 2200 m/s. Further, 500 steps of simulated annealing EM were performed with a target temperature at 0 K. Finally, a 20 ns MD simulation was performed at 298 K using a non-bonded cutoff of 7.86 Å. A snapshot was saved every 2.5 ps. For each peptide the binding energy was measured after proper energy minimization according to the following equation:

$$E_{\text{binding}} = \left(E_{\text{protein}} + E_{\text{ligand}}\right) - E_{\text{complex}}. \quad (2)$$

3. Results

3.1. BmooMPα-I is active upon neuro- and vaso-active peptides

In order to gain insights into BmooMPα-I substrate specificity, the enzyme was incubated with the neuro- and vaso-active peptides including angiotensin I, bradykinin, neurotensin, oxytocin, substance P and vasopressin. The sequence and cleavage sites of each assayed peptides are indicated in Table 1.

Despite the low primary sequence similarity among these peptides, a strong bias towards hydrolysis after proline residues was observed. BmooMPα-I cleaved oxytocin and bradykinin only after a proline residue in each sequence. Angiotensin I and Neurotensin were hydrolyzed at two positions, one having proline and the other containing aspartic acid and asparagine at P_1, respectively. Substance P was cleaved at least at five positions, one containing Pro at the P_1 position, and the others having Gln, Phe and Gly at this position. Among all assayed natural peptides, only vasopressin (NH_2-CYFQNC**P**RG-COOH) was resistant to BmooMPα-I hydrolysis, probably — due to its cyclic structure formed by the intramolecular disulfide bond between the two cysteine residues.

3.2. Substrate specificity of BmooMPα-I

In order to further evaluate the proteolytic activity of BmooMPα-I against proline-containing peptides and to determine its amino acid specificity, we synthesized and assayed FRET substrates based on the C-terminal sequence of human HMWK (high molecular weight kininogen) containing bradykinin segment 384–389 (…GFS**P**FR…). The peptide Abz-GFSPFRQ-EDDnp was taken as reference since it fulfilled three prerequisites for such analysis: (i) it contains only one proline residue in its sequence, (ii) the proline is located at the central position

Table 1
Hydrolysis of human proline-containing neuro- and vaso-active peptides by *BmooMPα-I*.[a]

Peptides	Sequence	Cleavage point by ESI-LCMS		
		Fragments	m/z	
			z = 1	z = 2
Angiotensin I	D↓RVYIH**P**↓FHL-NH_2	-RVYIH**P**-	783.9	391.9
		DRVYIH**P**FHL-NH_2	1296.5	648.2
Bradykinin	R**PP**GFS**P**↓FR	R**PP**GFS**P**-	756.9	378.5
		R**PP**GFS**P**FR	1060.2	530.1
Neurotensin	GlpLYEN↓K**P**↓RR**P**YIL	-K**P**-	243.3	–
Oxytocin	CYIQNC**P**↓LG-COOH	CYIQNC**P**-	839.9	419.9
		CYIQNC**P**LG-COOH	1010.2	505.1
Substance P	R**P**K**P**↓Q↓Q↓F↓FG↓LM-NH_2	R**P**K**P**-	496.6	248.3
		R**P**K**P**Q-	624.7	312.3
		R**P**K**P**QQF-	900.0	450.0
		R**P**K**P**QQFFG-	1104.3	552.1
		-QFFGLM-NH_2	741.9	–
		-FFGLM-NH_2	613.8	–
		-LM-NH_2	262.4	–
		R**P**K**P**QQFFGLM-NH_2	1348.6	674.3
Vasopressin	CYFQNC**P**RG (resistant)			

[a] Arrows indicate the cleavage bound determined by LCMS. Glp = pyroGlu.

of the peptide (flanked by three other amino acids at both C- and N-termini), and (iii) the cleavage site on this peptide was the same as in the natural bradykinin peptide, indicating that Abz and Q-EDDnp do not introduce restrictions or significant differences in the binding to BmooMPα-I.

The pH-profile of the hydrolytic activity of BmooMPα-I on Abz-GFSPFRQ-EDDnp as substrate was measured in the pH range from 4 to 10 (Fig. 1A) at constant ionic strength conditions. The hydrolysis rate values conform to "bell-shaped" pH rate profiles where very low activities were observed at extreme acid and basic pHs and the maximum activity was obtained at a slight basic pH (pH 7.9). BmooMPα-I has at least half of its maximum activity in the range from pH 6.7 ± 0.2 to 9.1 ± 0.1.

The effects of ionic strength on BmooMPα-I kinetic parameters of hydrolysis (k_{cat}, K_M and k_{cat}/K_M) of the peptide Abz-GFSPFRQ-EDDnp were analyzed by adding NaCl up to 1 M (Fig. 1B, C and D). Interestingly, the increase of NaCl concentration activated BmooMPα-I as observed by the increase in k_{cat}/K_M values resulted from systematic higher k_{cat} values, while the deviations on K_M were within the experimental error.

As described at [20], the inner-filter effect of the Abz-EDDnp compound impairs initial velocity data acquisition as substrate concentration is above 40 μM; an experimental condition that precludes the observation of true Michaelis–Menten kinetic parameters for FRET substrates having K_{Ms} higher than 20 μM. As observed in Fig. 1C, the K_M determined from Michaelis–Menten kinetics with velocity data up to 40 μM of Abz-GFSPFRQ-EDDnp was near to 25 μM in the absence of salt. In this case true specificity rate constants (k_{cat}/K_M) were determined by dividing the first-order rate constant measured at [S] ≪ K_M by the active enzyme concentration present in the reaction mixture [14]. Using this methodology, k_{cat}/K_M of this peptide in the same assay condition was 0.70 mM^{-1} s^{-1}.

The specificity rate constants (k_{cat}/K_M) of BmooMPα-I hydrolysis were determined assaying four series of peptides derived from the leader sequence Abz-GFSPFRQ-EDDnp. These series comprise a total of 21 peptides in which the P_2–P_1–P'_1–P'_2 residues (i.e., SPFR) were substituted by representatives of each class of natural amino acids (i.e., aliphatic, aromatic, polar, positively and negatively charged amino acids).

Table 2 shows the kinetic parameters for the hydrolysis of the peptide series Abz-GFSXFRQ-EDDnp with different amino acids at the X position. All substrates in these series were cleaved only at the X-Phe bond, indicating that X corresponds to the P_1 position. The catalytic efficiency of peptides with Ala, Qln and Glu was up to 5 times higher than observed with the reference peptide — that contains the proline residue at this position. The analogs with Asp and Arg were also hydrolyzed, while peptides containing aromatic resides (Trp and Phe) were resistant to hydrolysis.

All hydrolyzed substrates of the series Abz-GFXPFRQ-EDDnp were cleaved at the Pro–Phe bond (Table 2), indicating that X corresponds to the P_2 position. While the peptide containing the aliphatic amino acid Leu was preferred at this position, the peptides with Qln and Glu were also cleaved with k_{cat}/K_M values higher than the reference (that contains Ser at this position). Interestingly, the analog containing the positively charged side chain – Arg – was resistant to hydrolysis.

Table 3 shows the kinetic parameters for the hydrolysis of the peptide series Abz-GFSPXRQ-EDDnp and Abz-GFSPFXQ-EDDnp with different amino acids at the X position. All hydrolyzed substrates in the Abz-GFSPXRQ-EDDnp series were cleaved at the Pro-X bond, showing that X occupied the S'_1 subsite. A five-fold increase in the catalytic

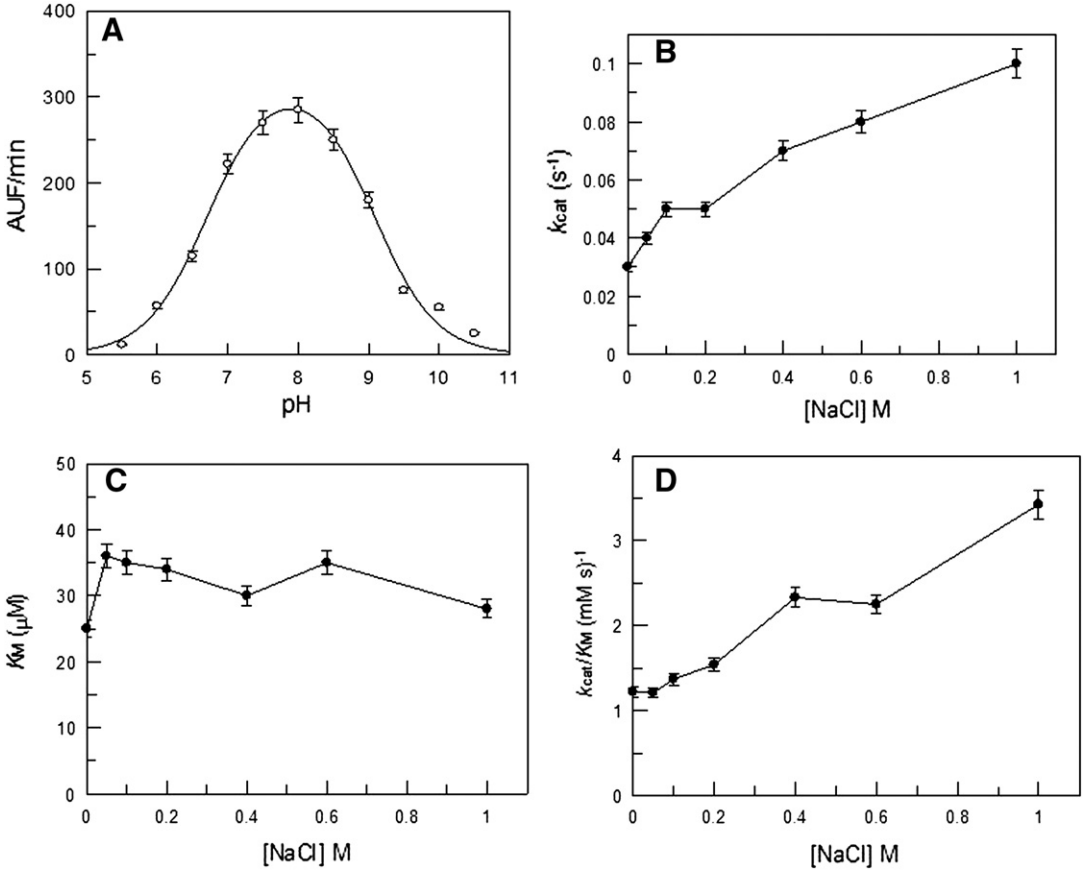

Fig. 1. NaCl effect and pH dependence BmooMPα-I proteolytic activity. (A) The pH profile was obtained by velocity of hydrolysis as Arbitrary Units of Fluorescence (AUF/min) in the standard buffer (75 mM Tris–HCl, 25 mM MES, 25 mM Acetic Acid and 25 mM Glycine) with 0.05 μM of enzyme and 10 μM $ZnCl_2$ with 2 μM Abz-GFSPFRQ-EDDnp as substrate. The effect of NaCl on catalytic parameters (B) k_{cat}, (C) K_M and (D) k_{cat}/K_M of hydrolysis of the peptide Abz-GFSPFRQ-EDDnp were measured as described in Materials and methods.

Table 2
Kinetic analysis for the hydrolysis of FRET Peptides Abz-GF**X**PFRQ-EDDnp and Abz-GFS**X**FRQ-EDDnp with variations (X) at positions P_2 and P_1, respectively.

	Abz-Peptidyl-EDDnp	k_{cat}/K_M $(mM \cdot s)^{-1}$
P_2	GF**L**P↓F**R**Q	1.17
	GF**Q**P↓F**R**Q	1.02
	GF**E**P↓F**R**Q	0.89
	GF**S**P↓F**R**Q	0.61
	GF**R**P F**R**Q	Resistant
P_1	GFS**A**↓F**R**Q	3.07
	GFS**Q**↓F**R**Q	2.72
	GFS**E**↓F**R**Q	2.60
	GFS**S**↓F**R**Q	1.48
	GFS**D**↓F**R**Q	0.67
	GFS**P**↓F**R**Q	0.61
	GFS**R**↓F**R**Q	0.45
	GFS**W**FRQ	Resistant
	GFS**F**FRQ	Resistant
	GFS**I**FRQ	Resistant

Table 4
Kinetic parameter for the hydrolysis of FRET peptide Abz-KLXPSKQ-EDDnp, with variations (X) at the P_2 position.

Abz-Peptidyl-EDDnp	k_{cat}/K_M $(mM \cdot s)^{-1}$
KL**E**P↓S**K**Q	0.58
KL**A**P↓S**K**Q	0.52
KL**D**P↓S**K**Q	0.49
KL**Q**P↓S**K**Q	0.40
KL**S**P↓S**K**Q	0.37
KL**L**P↓S**K**Q	0.36
KL**R**PSKQ	Resistant
KL**K**PSKQ	
KL**F**PSKQ	
KL**P**PSKQ	
KL**G**PSKQ	
KL**W**PSKQ	
KL**N**PSKQ	

efficiency of BmooMPα-I was observed with the substrate containing the aliphatic Leu at the P'_1 position. The analogs containing charged side chains (either Arg or Glu) as well as the peptide with the hydroxyl group of Ser at this position were resistant to hydrolysis. The low variance in the catalytic efficiency among Arg, Glu and Qln at the P'_2 position indicates a non-specific S'_2 subsite.

The substrate specificity of BmooMPα-I was assessed in details with the peptide series Abz-KLXPSKQ-EDDnp (Table 4). As expected, all cleaved peptides were hydrolyzed at the Pro–Ser bond confirming the tendency towards hydrolysis after proline residues. Peptides with small and negative charged residues were similarly hydrolyzed with k_{cat}/K_M values in the range of 0.36 (with Leu) to 0.58 $mM^{-1} \cdot s^{-1}$ (with Glu). The analogs containing the positively charged Arg and Lys, aromatic residues (Phe and Trp) as well as peptides Abz-KLPPSKQ-EDDnp, Abz-KLGPSKQ-EDDnp and Abz-KLNPSKQ-EDDnp were resistant to hydrolysis.

Interestingly, the peptide Abz-KLXPSKQ-EDDnp showed kinetic behavior similar to that observed with Abz-GFSXFRQ-EDDnp, in which K_M values were usually higher than 30 μM (data not shown) and the true k_{cat}/K_M was quite near to the value obtained with Abz-GFSPFRQ-EDDnp. The first observation supports the idea that the substrate promiscuity of BmooMPα-I is derived from the absence of strong contact points between substrate and enzyme subsites, and the latter suggests that while Pro position in the peptide determines the cleaved bond, its unique conformational constrains on the peptide chain also imposes a penalty in k_{cat}/K_M value.

Table 3
Kinetic analysis for the hydrolysis of FRET peptides Abz-GFSP**X**RQ-EDDnp and Abz-GFSPF**X**Q-EDDnp with variations (X) at positions P'_1 and P'_2 respectively.

	Abz-Peptidyl-EDDnp	k_{cat}/K_M $(mM \cdot s)^{-1}$	Relative Activity
P'_1	GFSP↓**L**RQ	3.04	100%
	GFSP↓**Q**RQ	0.99	33
	GFSP↓**F**RQ	0.61	20
	GFSP**S**RQ	Resistant	
	GFSP**E**RQ	Resistant	
	GFSP**R**RQ	Resistant	
P'_2	GFSP↓F↓**L**Q (P-F55%)	1.04	100%
	GFSP↓F**R**Q	0.61	59
	GFSP↓F**E**Q	0.44	42
	GFSP↓F**Q**Q	0.36	35

3.3. Screening of Abz-GXXZXXQ-EDDnp sublibraries

Synthetic combinatorial libraries (SCLs) of fluorogenic peptides, a strategy in which each position in the peptide sequence is occupied in turn by a single amino acid residue while the other positions are randomly occupied by one of the 20 natural amino acids have provided valuable information about the specificity of numerous peptidases [21]. Due to the large theoretical diversity of peptide sequences available for hydrolysis, SCLs are also pointed as a direct, efficient, and simple approach for the detection and initial characterization of endopeptidases.

Recently, we synthesized the fluorescence resonance energy transfer peptide library with the general structure Abz-GXXZXXQ-EDDnp, where X represents randomly incorporated amino acid residues (Cys was omitted to avoid sulfhydryl site reactions) and where the Z position is successively occupied with 1 of the 19 amino acids, resulting in 19 sublibraries each containing a theoretical diversity of approximately 100,000 peptides. The library was validated with the canonical peptidases trypsin, chymotrypsin, pepsin and cathepsin L and while almost all sublibraries were hydrolyzed by these peptidases, the differential rates of hydrolysis among them parallel the recognized specificity requirements known for each enzyme indicating that the Z position of Abz-GXXZXXQ-EDDnp was accommodated within the enzyme S_1 subsite [13].

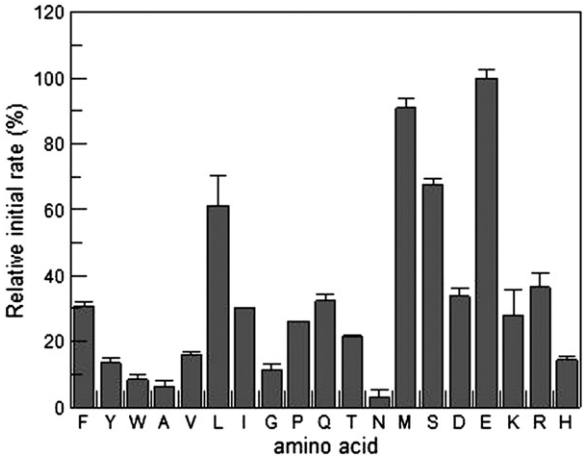

Fig. 2. Screening of the FRET combinatorial library Abz-GXXZXXQ-EDDnp. The X axis shows the fixed amino acid residues at the Z position, represented by single letter code. Relative activities were calculated as a percentage of the highest rates obtained. The errors are shown at the top of the bars, each of which represents the average of three determinations. Assays were performed as described under Materials and methods.

The contribution of each amino acid at the Z position to the initial rate of hydrolysis of the sublibraries was determined using BmooMPα-I concentration that exhibited a linear increase of the fluorescence with time and is shown in Fig. 2. While the best hydrolyzed sublibraries were those with Glu, Met, Leu and Ser at the Z position, the sublibrary Abz-GXXPXXQ-EDDnp described as resistant for canonical peptidases [13] was hydrolyzed with almost 30% of the activity found with Glu at the Z position.

In order to further confirm this view we synthesized the library MCA-GXXP↓XXQ-EDDnp. After incubation with BmooMPα-I, the product of hydrolysis was sequenced by Edman degradation. As MCA is resistant to the Edman degradation the number of cycles necessary to find Q of the Q-EDDnp residue will indicate the cleavage site. As expected, Q residue appeared in the third cycle of Edman degradation of all products of hydrolysis; thus the MCA-GXXPXXQ-EDDnp libraries are cleaved as indicated by the arrows, confirming BmooMPα-I as an unusual post-proline cleaving peptidase.

3.4. BmooMPα-I displays kininogenase activity

It was also investigated whether BmooMPα-I was able to cleave human high molecular weight kininogen, an essential protein of the kallikrein-kinin system (KKS) [22]. As shown in Fig. 3A, soluble HMWK migrated predominantly as a 120 kDa protein under reduced conditions on SDS-PAGE. After incubation with BmooMPα-I for 20 min, the intensity of the 120 kDa band was reduced and new bands appeared at 64–55, 45 and 15 kDa, similar to that reported in plasma and cells by the action of kallikrein, when bradykinin is liberated [23].

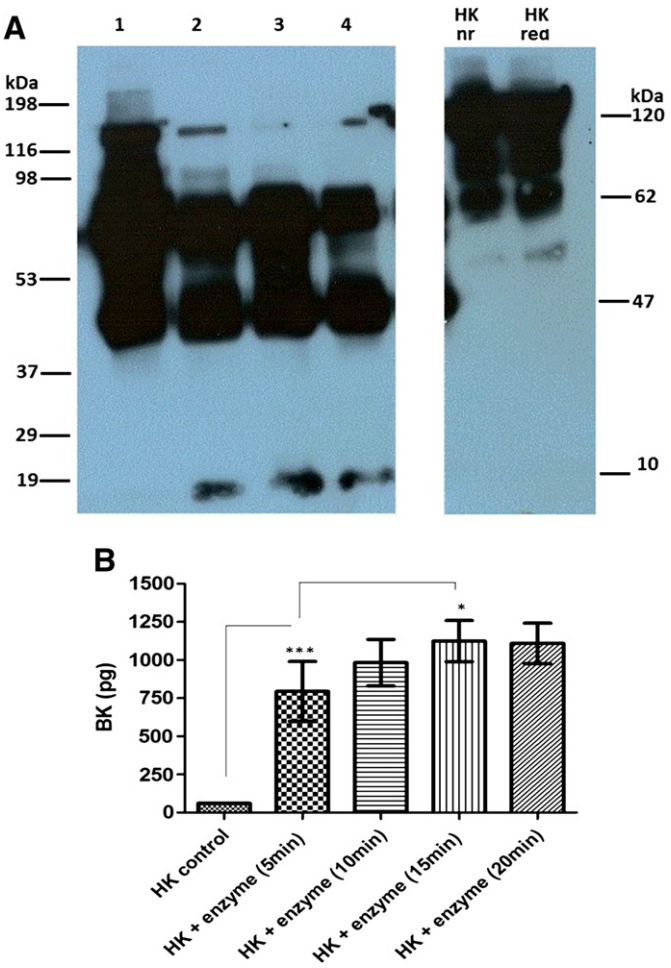

Fig. 3. BmooMPα-I kininogenase activity. (A) Degradation of HMWK (1.0 μg) by BmooMPα-I (1:1) was demonstrated by immunoblotting. The HMWK incubated with BmooMPα-I (lanes 1 — 5 min, 2 — 10 min, 3 — 15 min and 4 — 20 min) or without BmooMPα-I (HK nr and HK red (nr — no reduced and DTT HK reduced)) is shown. The cleavage products derived from HMWK (120 kDa) appeared as major bands of approximately 64–55, 45 and 15 kDa. Molecular mass standards and estimated molecular masses of the resolved proteins (kDa) are shown on the left and right of the figure, respectively. (B) Effect of BmooMPα-Ion bradykinin release. Bradykinin levels were determined by radioimmunoassay [29], in triplicate determinatives. Histograms show a significant BK release $^{*}p < 0.05$, $^{***}p < 0.001$.

The ability of BmooMPα-I to generate active kinins was also analyzed and quantified by radioimmunoassay using anti-bradykinin antibody. As observed in Fig. 3B, the enzyme was able to release kinins in ng range — similar to that observed with plasmatic kallikrein under the same experimental conditions [16]. In the presence of the metallopeptidase inhibitor, ortho-phenanthroline, the enzyme was unable to cleave the HMWK and release kinins (data not shown).

The kinin-releasing activity of BmooMPα-I was further analyzed using FRET peptides derived from the N- and C-terminal sequences of HMWK bradykinin-containing segment, Abz-MISLMKRPQ-EDDnp and Abz-GFSPFRSSRIQ-EDDnp, respectively. The first was hydrolyzed by BmooMPα-I at the S↓L (50%) and L↓M (50%) bonds with a k_{cat}/K_M of 6.85 $(mM \cdot s)^{-1}$ while the second was cleaved at the P↓F (10%) and R↓I (90%) bonds with a k_{cat}/K_M of 2.96 $(mM \cdot s)^{-1}$. The observed cleavage pattern in both peptides corroborates the ability of BmooMPα-I to release LMK-BK Leu-Met-Lys-bradykinin (LMKRPPGFSPFR) and Met-Lys-bradykinin (MKRPPGFSPFR) from HMWK. Protein–protein interactions between HMWK and BmooMPα-I could potentialize the cleavage to release Lys-bradykinin and/or bradykinin as observed in the radioimmunoassay using anti-bradykinin antibody. In fact, the observed promiscuity of BmooMPα-I also supports this hypothesis.

3.5. Structural basis for subsite specificity

Based on the three major subsites conferring specificity for BmooMPα-I (S_2, S_1 and S'_1 subsites) according to FRET peptide assays, we modeled the tripeptides LAL, LPL and LWL into the active-site pocket of the enzyme and performed energy minimization routines to identify the structural determinants for the enzyme ability to hydrolyze N-prolyl peptide bonds and to shed light on its amino acid selectivity. Binding energies corroborated with FRET peptide assays indicating a favorable binding for peptides having Ala at the P_1 position, followed by Pro and Trp, when having Leu at both P_2 and P'_1 positions (Table 5). The enzyme promiscuity observed in kinetic experiments comes from a naturally broadened active-site pocket, which can accommodate a variety of side chains in almost all subsites, with some restrictions at S_2, S_1 and S'_1 subsites. The geometry of the substrate channel along with the suggestion that the low selectivity derived from the absence of strong contact points between substrate R groups and the enzyme subsites may explain the ability of BmooMPα-I to cleave N-prolyl peptide bonds. The S_1 subsite is surrounded by the residues Arg108 and His150, which does not permit the binding of large aromatic side chains. In fact kinetic data showed that peptides having Trp and Phe residues at the P_1 position were resistant to hydrolysis. On the other hand, the S'_1 subsite consists of a voluminous pocket defined by the side chains of Ile106, Val136, His140 and Leu168, and the main-chain of residues forming the Met-turn (Fig. 4A and B), which explains the ability to accommodate large, hydrophobic or neutral, side chains such Leu, Qln and Phe. The hydrophobic

Table 5
Binding energies of the Leu-X-Leu tripeptides to BmooMPα-I.

Peptide sequence	Binding energy (kJ/Mol)
Leu-**Ala**-Leu	1123.7
Leu-**Pro**-Leu	615.2
Leu-**Trp**-Leu	545.3

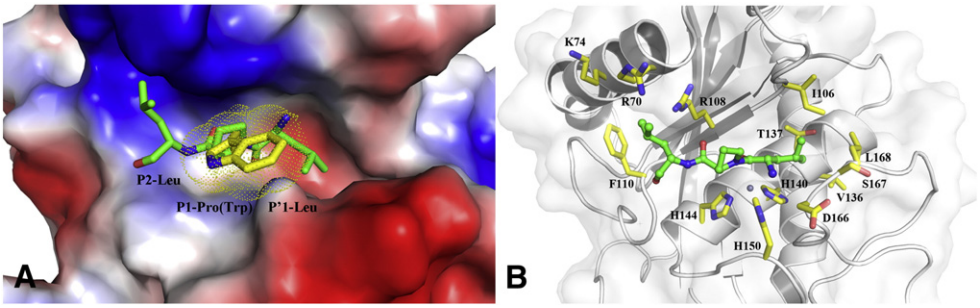

Fig. 4. Tri-peptide LP(W)L docked into BmooMPα-I structure. (A) Electrostatic surface representation of the active-site pocket (blue — positive, white — neutral and red — negative charge) with the van der Waals radius of the Trp side chain shown as dots, indicating steric clashes. (B) Cartoon representation of BmooMPα-I structure with the residues forming the subsites represented as sticks and balls (carbon colored in yellow). In both figures, the docked tripeptide LPL is drawn as sticks and balls with carbon atoms in green.

character of this subsite is not favorable for the binding of charged residues and its large volume may result in a lack of contacts with small side-chain residues, supporting FRET peptide assays. Interestingly, peptides having basic residues at the P_2 position were resistant to cleavage, which is caused by a repulsive electrostatic effect since this subsite is populated by basic residues (Arg70, Lys74 and Arg108) (Fig. 4A and B).

4. Discussion

Snake venom metalloproteinases orchestrate with other proteolytic enzymes a diversity of local and systemic reactions in the prey by molecular mechanisms still unclear. A dissection of the enzymatic properties of SVMPs including the best catalytic conditions, subsite specificity and physiological substrates is of great importance to a better understanding in the molecular processes triggered by these enzymes during envenomation and also can serve as a model tool for thrombosis and cardiovascular diseases.

Herein, we demonstrated that PI-class SVMP named as BmooMPα-I was able to cleave human proline-containing neuro- and vaso-active peptides including angiotensin I, bradykinin, neurotensin, oxytocin and substance P. Moreover, BmooMPα-I showed the interesting feature of cleaving most of these proline-containing peptides after the proline residue, which is unusual for most of characterized peptidases. Proline is the only genetically coded amino acid in proteins and its cyclized structure [24] confers a unique conformational constrain on the peptide chain. Thus, the discovery and comprehensive characterization of proline-specific enzymes are of great interest for both academic and industrial domains. In addition, the ability of BmooMPα-I to cleave Pro-X bonds suggests a functional correlation with mammalian prolyl oligopeptidases (POPs) that are involved in neurodegenerative and affective disorders, and probably in protein secretion and the phosphoinositide pathway [25].

The hydrolysis of proline-containing peptides was dissected by substrate specificity experiments, where BmooMPα-I showed a relatively high substrate promiscuity, accepting different amino acids at S_2–S'_2 subsites and potentially high K_M values (higher than 20 μM) for all assayed FRET substrates. The higher catalytic efficiency of peptides with Ala, Gln and Glu at the S_1 position indicates that while Pro presence in the peptide determines the scissile bond in both physiological and synthetic substrates, it also imposes a penalty in k_{cat}/K_M value. The screening of Abz-GXXZXXQ-EDDnp sublibraries confirm this result, with the Abz-GXXPXXQ-EDDnp, resistant for canonical peptidases, hydrolyzed after the Pro residue with almost 30% of the activity found with Glu at the Z position. These observations also support the azocaseinolytic and fibrin(ogen)olytic activities of BmooMPα-I since both the α chain of fibrinogen and casein are rich in proline residues.

In fact, structural analysis showed that BmooMPα-I has a broadened active-site cleft with only S_2, S_1 and S'_1 subsites providing some selectivity. This particular active-site geometry permits the binding of a variety of peptides even those with rigid configuration conferred by a proline residue at the P_1 position, which somehow is compensated by rearrangements of P_2, P'_1 and P'_2 residues reflecting in the suboptimal binding and lower catalytic efficiency when compared to peptides having Ala at the P_1 position.

While it is unclear if this post-proline cleaving activity is shared among other SVMPs, a proteome based approach points in this direction since proline was detected at the P_1 position of the cleavage sites of the P-I class SVMP leucurolysin-a from *Bothrops leucurus*, atrolysin C from *Crotalus atrox* and BaP1 from *Bothrops asper* [26]. Moreover, the metalloproteinases trimerelysin I (HR1A), HR2a and trimerelysin II (H2-proteinase) from *Trimeresurus flavoviridis* as well as Cbfib2 (*Crotalus basiliscus*) preferentially cleave the A α-chain of fibrinogen at the peptidyl bond of Pro516 and Met517 [27]. The metalloproteinase kaouthiagin from the cobra venom of *Naja kaouthia* cleaves the human VWF at a single peptide bond between Pro708 and Asp709 [28].

The kininogenase activity of BmooMPα-I here reported is also remarkable, since while several venom serine proteases have the activity for releasing bradykinin from kininogen [27] this activity that has not been assigned to the venom metalloproteases so far characterized. However, further studies are required to evaluate whether and how these activities are involved in the envenomation process.

Collectively, our results define BmooMPα-I as a post-proline cleaving peptidase and provided novel functional and structural information about snake venom metalloproteinases that might contribute to a further understanding in the molecular mechanisms governing the physiological effects of this important class of enzymes in the envenomation process.

Acknowledgements

This work was supported by grants from FAPESP- 2012/ 50191-4, CAPES and CNPq.

Appendix A. Supplementary data

Supplementary data to this article can be found online at http://dx.doi.org/10.1016/j.bbapap.2013.12.014.

References

[1] J.W. Fox, S.M.T. Serrano, Structural considerations of the snake venom metalloproteinases, key members of the M12 reprolysin family of metalloproteinases, Toxicon 45 (2005) 969–985.
[2] A.S. Kamiguti, C.R.M. Hay, R.D.G. Theakston, M. Zuzel, Insights into the mechanism of haemorrhage caused by snake venom metalloproteinases, Toxicon 34 (1996) 627–642.
[3] A.S. Kamiguti, M. Zuzel, R.D.G. Theakston, Snake venom metalloproteinases and disintegrins: interactions with cells, Braz. J. Med. Biol. Res. 31 (1998) 853–862.

[4] J.W. Fox, S.M.T. Serrano, Insights into and speculations about snake venom metalloproteinase (SVMP) synthesis, folding and disulfide bond formation and their contribution to venom complexity, FEBS J. 275 (2008) 3016–3030.
[5] J.M. Gutierrez, T. Escalante, A. Rucavado, Experimental pathophysiology of systemic alterations induced by *Bothrops asper* snake venom, Toxicon 54 (2009) 976–987.
[6] J.M. Gutierrez, A. Rucavado, T. Escalante, C. Diaz, Hemorrhage induced by snake venom metalloproteinases: biochemical and biophysical mechanisms involved in microvessel damage, Toxicon 45 (2005) 997–1011.
[7] P.K. Akao, C.C.C. Tonoli, M.S. Navarro, A.C.O. Cintra, J.R. Neto, R.K. Arni, M.T. Murakami, Structural studies of BmooMP alpha-I, a non-hemorrhagic metalloproteinase from *Bothrops moojeni* venom, Toxicon 55 (2010) 361–368.
[8] J.W. Fox, S.M.T. Serrano, Timeline of key events in snake venom metalloproteinase research, J. Proteome 72 (2009) 200–209.
[9] C.P. Bernardes, N.A. Santos, T.R. Costa, M.S.R. Gornes, F.S. Torres, J. Costa, M.H. Borges, M. Richardson, D.M. dos Santos, A.M.D. Pimenta, M.I. Homsi-Brandeburgo, A.M. Soares, F. de Oliveira, Isolation and structural characterization of a new fibrin(ogen) olytic metalloproteinase from *Bothrops moojeni* snake venom, Toxicon 51 (2008) 574–584.
[10] U.K. Laemmli, Cleavage of structural proteins during assembly of head of bacteriophage-T4, Nature 227 (1970) 680–685.
[11] E. Gasteiger, C. Hoogland, A. Gattiker, S. Duvaud, M.R. Wilkins, R.D. Appel, A. Bairoch, in: J.M. Walker (Ed.), The Proteomics Protocols Handbook, Humana Press, 2005, pp. 571–607.
[12] B. Korkmaz, S. Attucci, M.A. Juliano, T. Kalupov, M.L. Jourdan, L. Juliano, F. Gauthier, Measuring elastase, proteinase 3 and cathepsin G activities at the surface of human neutrophils with fluorescence resonance energy transfer substrates, Nat. Protoc. 3 (2008) 991–1000.
[13] L.C.G. Oliveira, V.O. Silva, D.N. Okamoto, M.Y. Kondo, S.M.B. Santos, I.Y. Hirata, M.A. Vallim, R.C. Pascon, I.E. Gouvea, M.A. Juliano, L. Juliano, Internally quenched fluorescent peptide libraries with randomized sequences designed to detect endopeptidases, Anal. Biochem. 421 (2012) 299–307.
[14] M.C. Araujo, R.L. Melo, M.H. Cesari, M.A. Juliano, L. Juliano, A.K. Carmona, Peptidase specificity characterization of C- and N-terminal catalytic sites of angiotensin I-converting enzyme, Biochemistry 39 (2000) 8519–8525.
[15] J.G. Andrezza, V.A. Nunes, A.K. Carmona, H.B. Nader, C.P. von Dietrich, V.L.F. Silveira, K. Shimamoto, N. Ura, M.U. Sampaio, C.A.M. Sampaio, M.S. Araujo, Glycosaminoglycans affect the action of human plasma kallikrein on kininogen hydrolysis and inflammation, Int. Immunopharmacol. 2 (2002) 1861–1865.
[16] S. Shimamoto, R. Moriyama, K. Sugimoto, S. Miyata, S. Makino, Partial characterization of an enzyme fraction with protease activity which converts the spore peptidoglycan hydrolase (SleC) precursor to an active enzyme during germination of *Clostridium perfringens* S40 spores and analysis of a gene cluster involved in the activity, J. Bacteriol. 183 (2001) 3742–3751.
[17] T. Lingott, C. Schleberger, J.M. Gutierrez, I. Merfort, High-resolution crystal structure of the snake venom metalloproteinase BaP1 complexed with a peptidomimetic: insight into inhibitor binding, Biochemistry 48 (2009) 6166–6174.
[18] E. Krieger, G. Koraimann, G. Vriend, Increasing the precision of comparative models with YASARA NOVA — a self-parameterizing force field, Proteins Struct. Funct. Genet. 47 (2002) 393–402.
[19] E. Krieger, T. Darden, S.B. Nabuurs, A. Finkelstein, G. Vriend, Making optimal use of empirical energy functions: force-field parameterization in crystal space, Proteins Struct. Funct. Genet. 57 (2004) 678–683.
[20] D.N. Okamoto, L.C.G. Oliveira, M.Y. Kondo, M.H.S. Cesari, M.A. Juliano, L. Polgar, L. Juliano, I.E. Gouvea, The increase of SARS-CoV 3CL peptidase activity due to macromolecular crowding effects in the milieu composition, Biol. Chem. 391 (2010) 1461–1468.
[21] B. Turk, Targeting proteases: successes, failures and future prospects, Nat. Rev. Drug Discov. 5 (2006) 785–799.
[22] S. Nagasawa, T. Nakayasu, Chemistry and Biology of the Kallikrein Kinin System in Health and Disease, DHEW Publication (NIH), Bethesda, Maryland, 1974.
[23] S. Schiffman, C. Mannhalter, K.D. Tyner, Human high molecular-weight kininogen — effects of cleavage by kallikrein on protein-structure and procoagulant activity, J. Biol. Chem. 255 (1980) 6433–6438.
[24] B.K. Kay, M.P. Williamson, P. Sudol, The importance of being proline: the interaction of proline-rich motifs in signaling proteins with their cognate domains, FASEB J. 14 (2000) 231–241.
[25] I. Brandt, S. Scharpe, A.M. Lambeir, Suggested functions for prolyl oligopeptidase: a puzzling paradox, Clin. Chim. Acta 377 (2007) 50–61.
[26] A.F. Paes Leme, T. Escalante, J.G. Pereira, A.K. Oliveira, E.F. Sanchez, J.M. Gutierrez, S.M. Serrano, J.W. Fox, High resolution analysis of snake venom metalloproteinase (SVMP) peptide bond cleavage specificity using proteome based peptide libraries and mass spectrometry, J. Proteomics 74 (2011) 401–410.
[27] T. Matsui, Y. Fujimura, K. Titani, Snake venom proteases affecting hemostasis and thrombosis, Biochim. Biophys. Acta Protein Struct. Mol. Enzymol. 1477 (2000) 146–156.
[28] J. Hamako, T. Matsui, S. Nishida, S. Nomura, Y. Fujimura, M. Ito, Y. Ozeki, K. Titani, Purification and characterization of kaouthiagin, a von Willebrand factor-binding and -cleaving metalloproteinase from *Naja kaouthia* cobra venom, Thromb. Haemost. 80 (1998) 499–505.
[29] A.J. Gozzo, V.A. Nunes, A.K. Carmona, H.B. Nader, C.P. von Dietrich, V.L.F. Silveira, K. Shimamoto, N. Ura, M.U. Sampaio, C.A.M. Sampaio, M.S. Araujo, Glycosaminoglycans affect the action of human plasma kallikrein on kininogen hydrolysis and inflammation, Int. Immunopharmacol. 2 (2002) 1861–1865.